Utilizing neutronics modelling to predict changing Pu ratios in UO2 in the presence of Th

Evitts, Lee; Gilbert, M. R. ; Middleburgh, Simon; Lee, Bill; Dahlfors, Marcus

Progress in Nuclear Energy

DOI:
https://doi.org/10.1016/j.pnucene.2021.103762

Published: 01/07/2021

Peer reviewed version

Utilizing neutronics modelling to predict changing Pu ratios in UO_2 in the presence of Th

L. J. Evitts[a,†], M. R. Gilbert[a,b] , S. C. Middleburgh[a], W. E. Lee[a,c] and M. Dahlfors[a]

[a]Nuclear Futures Institute, Bangor University, Gwynedd, LL57 2DG, United Kingdom
[b]AWE, Aldermaston, Reading, RG7 4PR, United Kingdom
[c]Institute for Security Science and Technology, Imperial College London, London, SW7 2AZ, United Kingdom

[†]Corresponding author: l.evitts@bangor.ac.uk

Abstract

The isotopic fractions of plutonium produced in a reactor are of significant value as nuclear forensic signatures, and the mechanisms of their production and alteration should be investigated thoroughly. A series of neutronics calculations were made on a typical UO_2 PWR setup, introducing (Th, U)O_2 MOX rods gradually, to investigate how the presence of Th affects the $^{240}Pu/^{239}Pu$ and $^{242}Pu/^{239}Pu$ ratios in the remaining UO_2 fuel rods. A relationship is found that links the percentage change in these ratios, with the burnup and Th content in the configuration. In an extreme case, it was found that the presence of Th may increase the ratio of $^{242}Pu/^{239}Pu$ by as much as 3.5 % at low burnup.

Keywords

Nuclear forensics, thorium-based fuels, neutronics modelling, plutonium fingerprints, advanced fuels.

1. Introduction

In the production of plutonium in a nuclear reactor, the isotopic composition of the plutonium has been shown to be heavily dependent on the neutron energy spectrum experienced by the uranium under irradiation [1,2]. This neutron energy distribution is a function of several factors, including the initial ^{235}U enrichment, however the largest individual effect comes from the moderating material used within the reactor [2–4]. As such, the isotopic composition of plutonium produced will differ between different reactor types, with this variation becoming increasingly pronounced with increasing burnup [2,4–6]. Within the field of nuclear forensics, the correlations between different plutonium isotope ratios have been historically used to create isotopic fingerprints of plutonium produced by different reactor types, which have provided valuable signatures in ascribing the provenance of plutonium materials of unknown origin [7–10]. For example, in Figure 1 a distinguishing fingerprint is shown by plotting the $^{242}Pu/^{239}Pu$ ratio against the $^{240}Pu/^{239}Pu$ ratio for all major commercial reactor types [11].

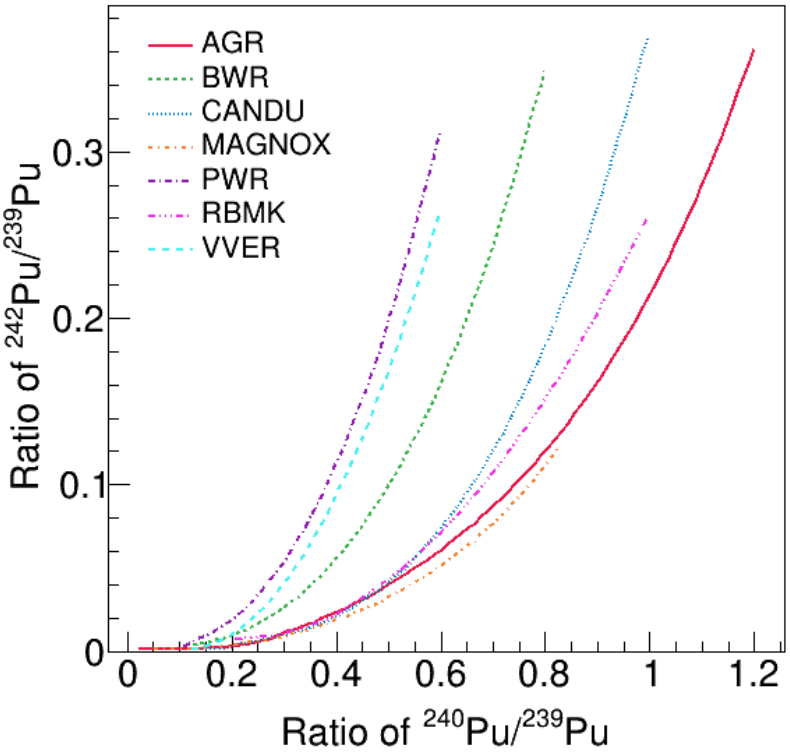

Figure 1: Representative Pu isotopic fingerprints for different reactor types, based on PIE data from SFCOMPO database [11]. The fingerprints shown are for a typical Boiling Water Reactor (BWR), Pressurized Water Reactor (PWR), Water-Water Energetic Reactor (VVER), Advanced Gas-cooled Reactor (AGR), Canadian Deuterium Uranium (CANDU) reactor, and the High-power Channel-type Reactor (RBMK)

However, with new and advanced fuel designs nearing commercial use, the contribution of the fuel materials themselves to the plutonium isotopic composition is becoming increasingly important, and particularly in the case of mixed and composite fuels. For example, Post-Irradiation Examination (PIE) data of plutonium produced from (U, Pu)O_2 Mixed OXide (MOX) fuelled Light Water Reactors (LWRs) has shown their isotopic fingerprint to be clearly distinguishable from that of UO_2 fuelled LWRs [11]. The increased use of dopants, such as in some Accident Tolerant Fuel (ATF) concepts, or other fissile or fertile elements, will also influence the plutonium isotopic composition [12].

Thorium-based fuels are a prominent example of fuel material influencing the plutonium isotopic composition. While ^{232}Th does not breed plutonium itself, it is a fertile as opposed to fissile isotope, hence requires a fissile 'driver' within the fuel [13]. Thorium fuels are therefore often in the form of MOX fuels such as (Th, U)O_2, which may be found in homogeneous or heterogeneous forms depending on the costs, neutronics, and burnable poison requirements [14–18]. In the MOX fuels plutonium will still be produced from the irradiation of the uranium component. However, the higher thermal absorption cross-section of ^{232}Th (relative to ^{238}U) leads to a greater production of ^{233}U in thorium-based fuels over uranium-based fuels which, in turn, produces a higher fission neutron yield than ^{239}Pu [19,20]. As such, the uranium component of the fuel will experience a different neutron energy distribution to that of a nominally pure UO_2 fuel, and so alter the isotopic composition of fission and transmutation products, including plutonium.

What is as yet poorly understood, is the magnitude of this effect on the plutonium isotopic composition, and hence its divergence from the commonly understood isotopic fingerprints of different reactor types. Such divergence, were it to be significantly observable, could result in additional forensic signatures to support the provenance assessment of plutonium materials, or

alternatively, obfuscate those already existing signatures so that they are no longer valid. This study represents one of the first such examinations of these effects, using neutronics calculations to investigate the changes in isotopic composition of plutonium produced as a function of Th content and burnup, and therefore how these changes may support the identification of the potential origin of plutonium materials.

2. Methodology

The Serpent 2.1.31 Monte Carlo code [21], utilizing the JEFF3.1 data libraries [22], was used to simulate the burnup of an axially infinite 17 x 17 PWR. A PWR is a well understood and modelled system, and also crucially one for which the Pu isotopic fingerprints arising from both UO_2 and $(U,Pu)O_2$ MOX fuels have been well studied [5–7,10], and as such provides an excellent baseline dataset for comparison. The Chebyshev Rational Approximation Method [23] was used to simulate burnup in the materials of interest. Each iteration of the Serpent code is tested against the results of MCNP [24] calculations, and previous publications have performed their own validity testing [25–27] so no benchmark calculations are performed here. A set of 45 calculations were performed in 2D parameter space, varying both:

i) The number of UO_2 fuel rods that are substituted with homogeneous $(Th, U)O_2$ MOX rods (1, 2, …, 9).
ii) The ThO_2 molar weight of the MOX rods (10 %, 20 %, …, 50 %).

Ten calculations were performed for each combination of parameters, randomizing the position of the MOX fuel rods each time. In each calculation the fuel rods remain in position for the duration of the burnup while the decay of any produced radionuclides are simulated. An average result was calculated from the set of ten to remove positional bias. The randomisation of the rods was restricted to ensure they were not placed within two spots of one another or to the edge of the assembly (primarily due to the periodic boundary conditions in place). The standard error in the mean was calculated for the nuclide quantities. An example randomization is shown in Figure 2 The first, second and third nearest neighbours to the red MOX rods have been identified for an investigation of nearby behaviour.

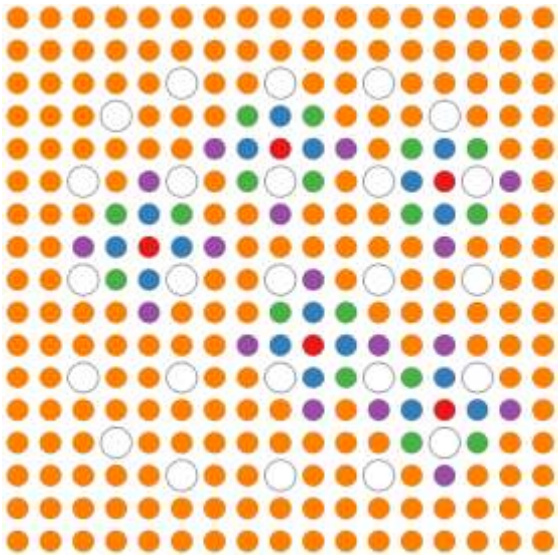

Figure 2: Example randomization of five MOX rods (red) within a 17 x 17 PWR. The orange rods are standard UO_2, while the blue, green and purple rods are the first, second and third nearest UO_2 neighbours to the MOX rods, respectively. The large white circles are the guiding tubes.

All rods are enclosed with a zirconium alloy cladding, including the guide tubes. The densities of the MOX rods are linearly extrapolated from experimental data [28,29]. The International Criticality Safety Benchmark Evaluation Project (ICSBEP) [30] is a database containing safety benchmark specifications, from which typical parameters and geometries of a PWR were extracted and detailed in Table 1. The ratio of Th isotopes is defined by natural abundances whereas the enrichment of U in a PWR can be as much as 5 %, therefore calculations are performed at 3 % and 5 % enrichments in order to sample this spread. Rotationally symmetric periodic boundary conditions are enabled. A number of calculations were run, increasing the neutron population number until the statistical precision was satisfactory. Each calculation in this work were therefore run with 100 active and 20 inactive cycles with 10,000 neutrons in each.

Table 1: Input parameters and geometries of a typical PWR used in this work.

Assembly	
Array	17 x 17
Fuel rod pitch (mm)	12.65
Fuel assembly pitch (mm)	215
Power density (W/g)	38.6
Fuel Rods	
^{235}U enrichment (%)	3 and 5
Density [UO_2] (g/cm^3)	10.97
Density [(Th, U)O_2] (g/cm^3)	10.47 to 10.87, depending on amount of ThO_2 present
Temperature (K)	900
Outer radius (mm)	4.126
Cladding	
Material	Zircaloy-4 [31]
Density (g/cm^3)	6.56

Temperature (K)	600
Inner radius (mm)	4.126
Outer radius (mm)	4.74
Coolant	
Material	Light water w/ 550 ppm of boron
Density (g/cm^3)	2.12
Temperature (K)	600

3. Results & Discussion

The effective neutron multiplicative factor for the assembly with the axially infinite rods, k_∞, was investigated for two extreme conditions at the two uranium enrichment values. In the first case, the calculation is for an assembly containing only UO_2 rods with no Th present, while in the second case, the calculation includes nine MOX rods, each with a ThO_2 weighting of 50 %. The results of the two cases are shown in Figure 3, where the burnup range is limited to the appropriate value based on the level of enrichment i.e. 30 MWd/kgU for 3 % and 50 MWd/kgU for 5 % enrichment. In both cases, the k_∞ begins at a value above unity and decreases as a function of burnup, as is typical particularly as there are no burnable absorbers present in the simulation [32]. The absolute difference in the reactivity between the UO_2 and (U, Th)O_2 cases, $|\Delta\rho|$, varies between 500 and 800 pcm, highlighting that the insertion of Th affects the neutron yield in the reactor.

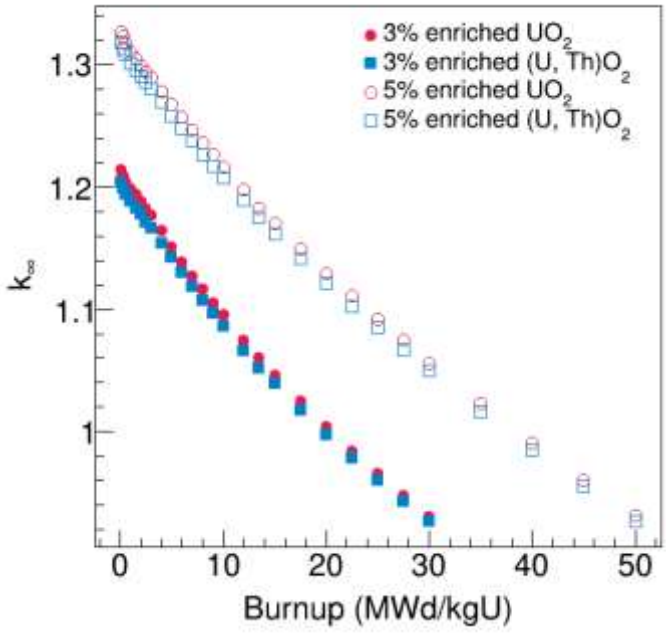

Figure 3: The effective neutron multiplicative factor for the axially infinite fuel rods, k_∞, for two calculation sets; one with no MOX rods present (red) and with nine MOX rods with a ThO_2 weighting of 50% substituted, for the two enrichment values.

The fractional amount of $^{238\text{-}242}$Pu, starting at 0.1 MWd/kgU and increasing as a function of burnup, is shown in the top panel of Figure 4 for standard 3 % enriched UO_2 (when no MOX rods are present in the assembly) and MOX fuel rods when they are inserted. The behaviour shown in Figure 4 is typical of a UO_2 fuel rod [33]. When Th is included in the fuel to create a MOX rod, it can be seen that the isotopic ratios of Pu change as a function of burnup. For example, the fractional amount of ^{240}Pu

decreases whilst ^{242}Pu increases, relative to the UO_2 fuel rods. In the bottom panel of Figure 4, the average of the standard UO_2 fuel rods in the MOX assembly are compared with the UO_2 rods that are positioned adjacent (first nearest neighbour, shown as blue in Figure 2) to the MOX rods to understand the impact of proximity. Similar trends to those that are occurring within the MOX rods themselves are observed in the adjacent UO_2 rods, though the deviations are of a smaller magnitude. At this scale there is no observable difference between the standard UO_2 and the weighted average of all UO_2 fuel rods within the MOX calculation.

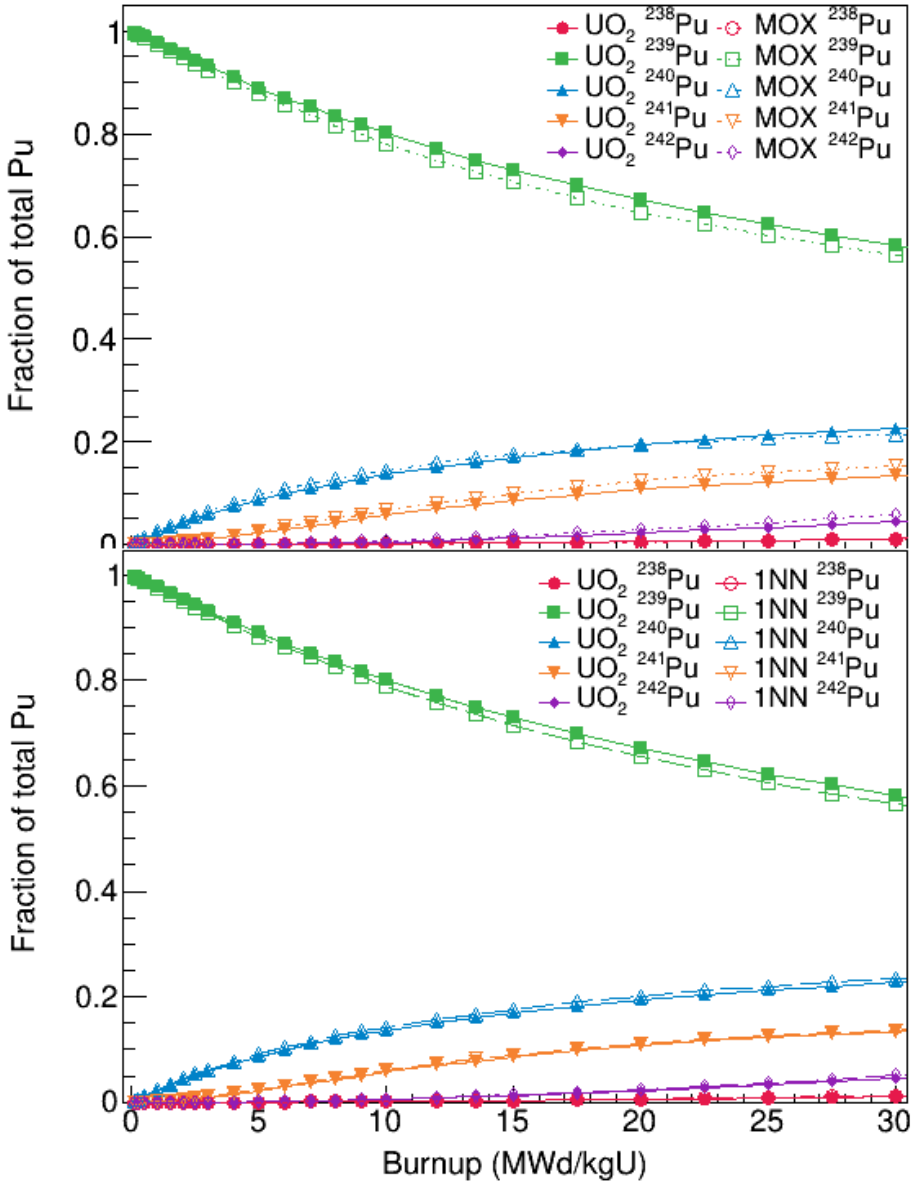

Figure 4: Fractional amount of Pu, as a function of burnup, for fuel rod calculations. The amount observed in standard 3% enriched UO_2 fuel is compared with (top) MOX fuel and (bottom) UO_2 fuel that is adjacent to the MOX (denominated '1NN'). The values begin at 0.1 MWd/kgU. The parameters of the calculation were chosen such that the error bars here would be insignificant.

The $^{242}Pu/^{239}Pu$ to $^{240}Pu/^{239}Pu$ relationship is shown in Figure 5 for the average result of specific pins:

i) The 3 % enriched UO_2 fuel rods when no Th is present in the assembly.
ii) The (Th, U)O_2 MOX rods when nine are present in the assembly, each with a ThO_2 molar weight of 50 %.
iii) The UO_2 fuel rods that are the first nearest neighbour (1NN) to the MOX rods described in (ii).

As burnup increases along the curve, the difference between (i) and (ii) is quite clear, as the ratio of $^{240}Pu/^{239}Pu$ remains lower in the MOX than in the standard UO_2 fuel. However, as in Figure 4, only minute deviations may be observed between the UO_2 fuel rods in the two different assembly configurations, (i) and (iii). However, the difference may be observed in the averaged UO_2 fuel rods in Figure 6, where the ratio of $^{242}Pu/^{239}Pu$ is plotted as a function of the number of MOX fuel rods present in the assembly. It can be seen that the ratio increases as a function of the number of rods and the Th weighting, i.e. the amount of Th present increases the ratio observed in the surrounding UO_2 fuel rods.

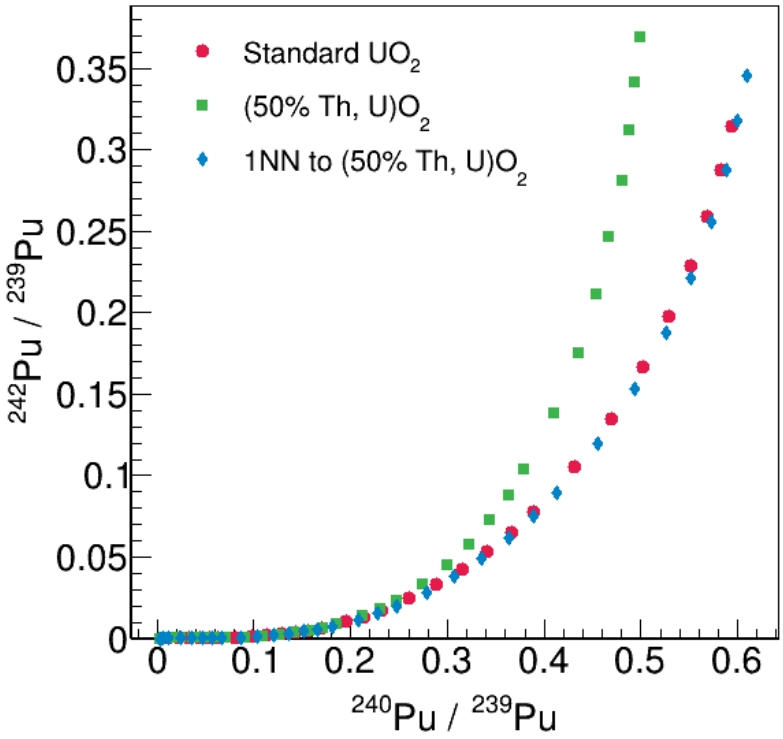

Figure 5: The relationship between $^{242}Pu/^{239}Pu$ and $^{240}Pu/^{239}Pu$ for a standard 3% enriched UO_2 fuel rod, a MOX rod with a ThO_2 weighting of 50 %, and the first nearest neighbour (1NN) to the previous MOX rod.

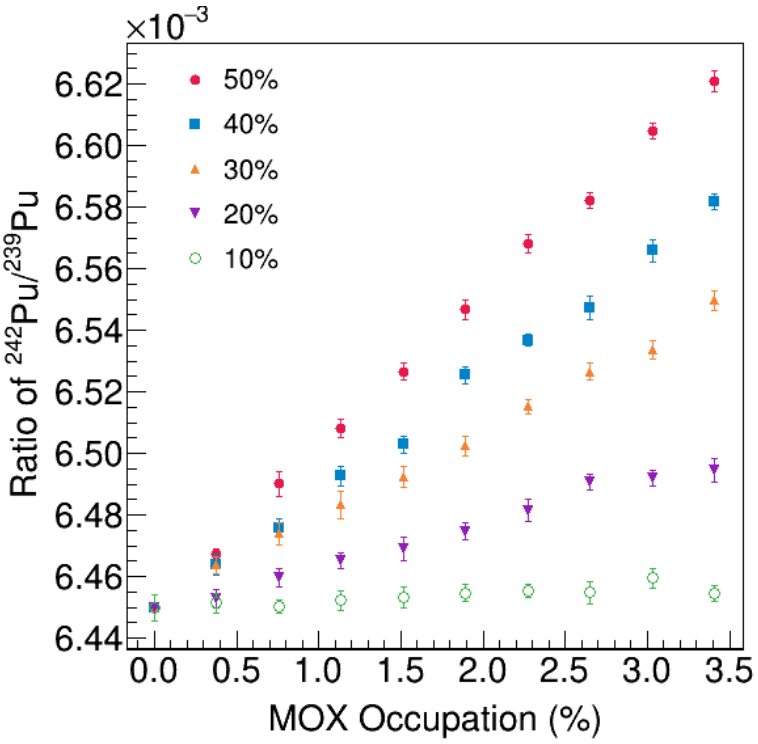

Figure 6: The ratio of $^{242}Pu/^{239}Pu$ in the 3% enriched UO_2 fuel rods that are exposed to different Th weightings of the MOX fuel, at a burnup of 10 MWd/kgU.

The number of substituted MOX rods and the Th weighting is folded into one parameter; the Th content, *t*, is the relative amount of Th in the entire assembly and is calculated from the fractional amount of MOX substitutions multiplied by the mass percentage. The percentage change of the $^{240}Pu/^{239}Pu$ and $^{242}Pu/^{239}Pu$ ratios in the averaged UO_2 fuel rods, relative to the standard 3 % enriched UO_2 calculation (i.e. with no Th present in the assembly), *P*, are shown in Figures 7 and 8 as a function of the Th content and the burnup, *b*, of the material. A second/third order polynomial surface, i.e.

$$P\ (\%) = \sum_{x=0}^{1}\sum_{y=0}^{2} C_{xy} b^x t^y$$

is fit to the data. The form of the fit was determined by minimizing both the reduced χ^2 value and the number of coefficients, C_{xy}, used and it was found that C_{02} is zero in all fits. The initial U enrichment does not significantly alter the Pu ratios, thus only the 3 % enriched calculations are shown in Figures 7 and 8. At low burnup and high Th content, the $^{242}Pu/^{239}Pu$ change is as high as 3.5 % and 3.1 % for the 3 % and 5 % initial U enrichments, respectively, while the $^{240}Pu/^{239}Pu$ change is around 1.2 % for both initial U enrichments. The change then decreases as Th content decreases and burnup increases. The parameters of the fit for both levels of enrichment calculated, along with their errors, are shown in Table 2. The reduced χ^2 value shows that the sum of residuals is low for each fit.

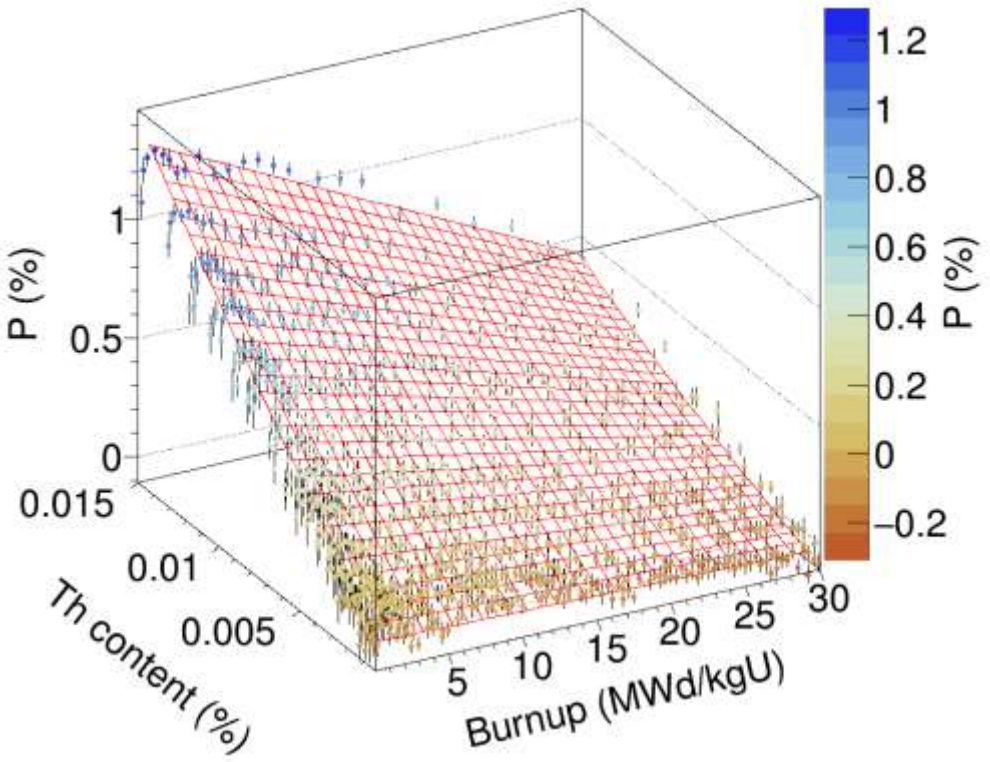

Figure 7: Percentage change, P, of $^{240}Pu/^{239}Pu$ in averaged 3 % enriched UO_2 rods under the presence of Th, and as a function of burnup.

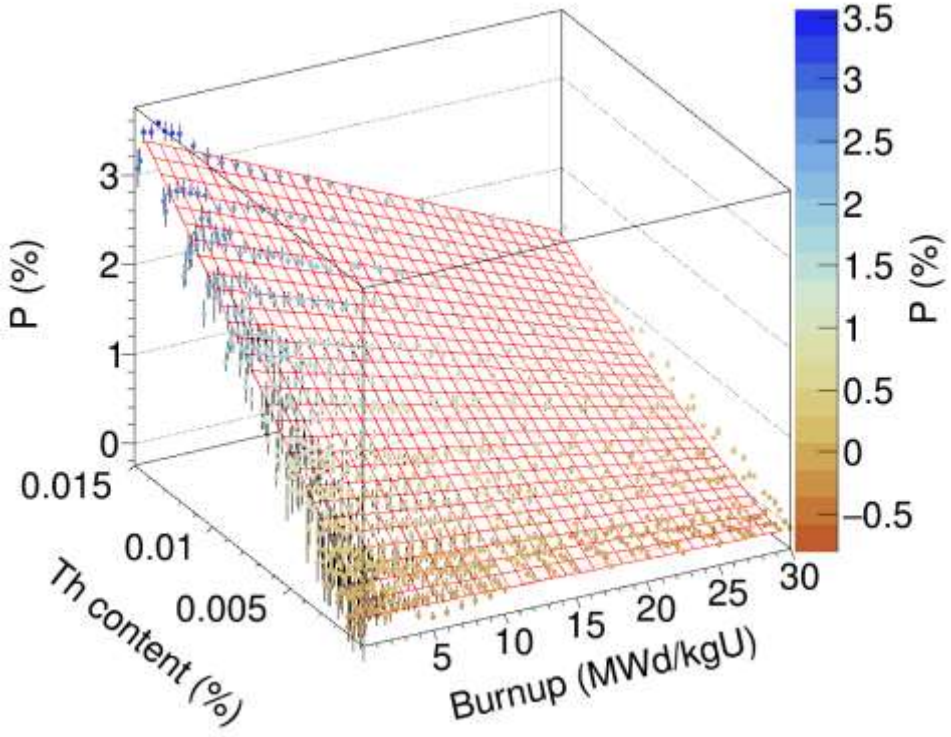

Figure 8: Percentage change, P, of $^{242}Pu/^{239}Pu$ in averaged 3 % enriched UO_2 rods under the presence of Th, and as a function of burnup.

Table 2: Parameters of the fit for Equation 1, relating the burnup and Th content to the percentage increase in Pu ratios.

	3% Enrichment		5% Enrichment	
Parameter	**$^{240}Pu/^{239}Pu$**	**$^{242}Pu/^{239}Pu$**	**$^{240}Pu/^{239}Pu$**	**$^{242}Pu/^{239}Pu$**
C_{00}	-0.050(2)	-0.096(3)	-0.055(2)	-0.086(3)
C_{01}	0	239.6(7)	0	227.5(5)
C_{02}	0	0	0	0
C_{10}	85(1)	0	68.5(9)	0
C_{11}	620(70)	-6.03(5)	1070(70)	-3.52(3)
C_{12}	-2.04(1)	82(5)	-0.547(12)	80(3)
Reduced χ^2	3.9	7.6	4.3	10.7

4. Conclusion

Through neutronics calculations, the ratios of $^{240}Pu/^{239}Pu$ and $^{242}Pu/^{239}Pu$ have been investigated in UO_2 pellets, as a function of Th content, U enrichment and burnup in a typical Pressurized Water Reactor (PWR), when MOX rods are substituted into the reactor. It is shown that the ratios do change in the UO_2 fuel rods, particularly in the adjacent fuel rods. A relationship is determined that links the percentage change in the UO_2 rods, with the burnup and Th content, which may be utilized in nuclear forensic studies. Overall, the uranium enrichment does not significantly impact the results. However, whilst the percentage change in the remaining UO_2 fuels may be less than a percent at high burnup values, a significant 3.5% and 3.1% change in $^{242}Pu/^{239}Pu$ is observed at low burnup and a high Th content for initial uranium enrichments of 3% and 5%, respectively, providing a potential means of discriminating thorium fuel use in such low burnup situations.

The $^{242}Pu/^{239}Pu$ to $^{240}Pu/^{239}Pu$ isotopic fingerprint of the (Th, U)O_2 MOX can be clearly distinguished from that of the UO_2 due to the increased $^{242}Pu/^{239}Pu$ and decreased $^{240}Pu/^{239}Pu$ ratios in the MOX compared to the UO_2. Therefore, in this instance the (Th, U)O_2 MOX fingerprint is well resolved from all those of standard UO_2 fuel, and would not overlap with those of a different reactor types in Figure 1. However, for other reactor types in which the use of (Th, U)O_2 is proposed, such as Pressurized Heavy Water Reactors (PHWR), a similar shift in $^{242}Pu/^{239}Pu$ to $^{240}Pu/^{239}Pu$ relationship could result in overlap with the LWRs and so potential mis-identification of reactor type. As such, this demonstrates a new potential signature to aid in ascribing the provenance of plutonium materials and underlines the importance of accounting for the effects of fuel composition, highlighting a new avenue for future nuclear forensics simulations to explore.

Acknowledgements

This work was carried out as part of the Sêr Cymru II programme funded through the Welsh European Funding Office (WEFO) under the European Development Fund (ERDF). Computing resources were made available by HPC Wales and Supercomputing Wales and special thanks are due to Aaron Owen, Benjamin Nash and Adrian Fewings.

References

[1] M. Wallenius, P. Peerani, and L. Koch, *Origin Determination of Plutonium Material in Nuclear Forensics*, J. Radioanal. Nucl. Chem. **246**, 317 (2000).

[2] A. T. Luksic, B. A. Collins, J. I. Friese, J. M. Schwantes, J. R. Starner, and J. F. Wacker, Isotopic Measurements: Interpretation and Implications of Plutonium Data, No. PNNL-SA--73572, Pacific Northwest National Laboratory, 2010.

[3] K. Mayer, M. Wallenius, and I. Ray, *Nuclear Forensics—a Methodology Providing Clues on the Origin of Illicitly Trafficked Nuclear Materials*, Analyst **130**, 433 (2005).

[4] A. Glaser, *Isotopic Signatures of Weapon-Grade Plutonium from Dedicated Natural Uranium–Fueled Production Reactors and Their Relevance for Nuclear Forensic Analysis*, Nucl. Sci. Eng. **163**, 26 (2009).

[5] M. Robel and M. J. Kristo, *Discrimination of Source Reactor Type by Multivariate Statistical Analysis of Uranium and Plutonium Isotopic Concentrations in Unknown Irradiated Nuclear Fuel Material*, J. Environ. Radioact. **99**, 1789 (2008).

[6] G. Nicolaou and S. R. Biegalski, *Discrimination of Plutonium from Thermal Reactors in the Frame of Nuclear Forensics*, J. Radioanal. Nucl. Chem. **317**, 559 (2018).

[7] G. Nicolaou, *Determination of the Origin of Unknown Irradiated Nuclear Fuel*, J. Environ. Radioact. **86**, 313 (2006).

[8] M. Wallenius, K. Lützenkirchen, K. Mayer, I. Ray, L. A. de las Heras, M. Betti, O. Cromboom, M. Hild, B. Lynch, A. Nicholl, H. Ottmar, G. Rasmussen, A. Schubert, G. Tamborini, H. Thiele, W. Wagner, C. Walker, and E. Zuleger, *Nuclear Forensic Investigations with a Focus on Plutonium*, J. Alloys Compd. **444–445**, 57 (2007).

[9] G. Nicolaou, *Provenance of Unknown Plutonium Material*, J. Environ. Radioact. **99**, 1708 (2008).

[10] I. Lantzos, C. Kouvalaki, and G. Nicolaou, *Plutonium Fingerprinting in Nuclear Forensics of Spent Nuclear Fuel*, Prog. Nucl. Energy **85**, 333 (2015).

[11] F. Michel-Sendis, I. Gauld, J. S. Martinez, C. Alejano, M. Bossant, D. Boulanger, O. Cabellos, V. Chrapciak, J. Conde, I. Fast, M. Gren, K. Govers, M. Gysemans, V. Hannstein, F. Havlůj, M. Hennebach, G. Hordosy, G. Ilas, R. Kilger, R. Mills, D. Mountford, P. Ortego, G. Radulescu, M. Rahimi, A. Ranta-Aho, K. Rantamäki, B. Ruprecht, N. Soppera, M. Stuke, K. Suyama, S. Tittelbach, C. Tore, S. V. Winckel, A. Vasiliev, T. Watanabe, T. Yamamoto, and T. Yamamoto, *SFCOMPO-2.0: An OECD NEA Database of Spent Nuclear Fuel Isotopic Assays, Reactor Design Specifications, and Operating Data*, Ann. Nucl. Energy **110**, 779 (2017).

[12] J. Arborelius, K. Backman, L. Hallstadius, M. Limbäck, J. Nilsson, B. Rebensdorff, G. Zhou, K. Kitano, R. Löfström, and G. Rönnberg, *Advanced Doped UO2 Pellets in LWR Applications*, J. Nucl. Sci. Technol. **43**, 967 (2006).

[13] W. E. Lee, M. Gilbert, S. T. Murphy, and R. W. Grimes, *Opportunities for Advanced Ceramics and Composites in the Nuclear Sector*, J. Am. Ceram. Soc. **96**, 2005 (2013).

[14] A. Galperin, E. Shwageraus, and M. Todosow, *Assessment of Homogeneous Thorium/Uranium Fuel for Pressurized Water Reactors*, Nucl. Technol. **138**, 111 (2002).

[15] J. S. Herring, P. E. MacDonald, K. D. Weaver, and C. Kullberg, *Low Cost, Proliferation Resistant, Uranium–Thorium Dioxide Fuels for Light Water Reactors*, Nucl. Eng. Des. **203**, 65 (2001).

[16] M. Saglam, J. J. Sapyta, S. W. Spetz, and L. A. Hassler, *Core Designs and Economic Analyses of Homogeneous Thoria-Urania Fuel in Light Water Reactors*, Nucl. Technol. **147**, 8 (2004).

[17] M. Todosow, A. Galperin, S. Herring, M. Kazimi, T. Downar, and A. Morozov, *Use of Thorium in Light Water Reactors*, Nucl. Technol. **151**, 168 (2005).

[18] M. Saoudi, D. Staicu, J. Mouris, A. Bergeron, H. Hamilton, M. Naji, D. Freis, and M. Cologna, *Thermal Diffusivity and Conductivity of Thorium- Uranium Mixed Oxides*, J. Nucl. Mater. **500**, 381 (2018).

[19] M. S. Kazimi, K. R. Czerwinski, M. J. Driscoll, P. Hejzla, and J. E. Meyer, ON THE USE OF THORIUM IN LIGHT WATER REACTORS, No. MIT-NFC-TR-016, Massachusetts Institute of Technology, 1999.
[20] Thorium Fuel Utilization: Options and Trends, No. IAEA-TECDOC-1319, International Atomic Energy Agency, 2002.
[21] J. Leppänen, M. Pusa, T. Viitanen, V. Valtavirta, and T. Kaltiaisenaho, *The Serpent Monte Carlo Code: Status, Development and Applications in 2013*, Ann. Nucl. Energy **82**, 142 (2015).
[22] OECD/NEA Data Bank, The JEFF-3.1 Nuclear Data Library, No. 21, 2006.
[23] P. Maria, *Higher-Order Chebyshev Rational Approximation Method and Application to Burnup Equations*, Nucl. Sci. Eng. **182**, 297 (2016).
[24] Los Alamos Scientific Laboratory. Group X-6, *MCNP : A General Monte Carlo Code for Neutron and Photon Transport* (Los Alamos, N.M. : Dept. of Energy, Los Alamos Scientific Laboratory ; [Springfield, Va.] : [for sale by the National Technical Information Service], 1979., 1979).
[25] Y. Lu, G. Zhou, F. A. Hernández, P. Pereslavtsev, J. Leppänen, and M. Ye, *Benchmark of Serpent-2 with MCNP: Application to European DEMO HCPB Breeding Blanket*, Fusion Eng. Des. **155**, 111583 (2020).
[26] J. Jang, W. Kim, S. Jeong, E. Jeong, J. Park, M. Lemaire, H. Lee, Y. Jo, P. Zhang, and D. Lee, *Validation of UNIST Monte Carlo Code MCS for Criticality Safety Analysis of PWR Spent Fuel Pool and Storage Cask*, Ann. Nucl. Energy **114**, 495 (2018).
[27] D. Ćalić, G. Žerovnik, A. Trkov, and L. Snoj, *Validation of the Serpent 2 Code on TRIGA Mark II Benchmark Experiments*, Appl. Radiat. Isot. **107**, 165 (2016).
[28] W. Rüdorff and G. Valet, *Über das Ceruranblau und Mischkristalle im System CeO2-UO2-U3O8*, Z. Für Anorg. Allg. Chem. **271**, 257 (1953).
[29] M. Murabayashi, S. Namba, Y. Takahashi, and T. Mukaibo, *Thermal Conductivity of ThO2-UO2 System*, J. Nucl. Sci. Technol. **6**, 128 (1969).
[30] NEA, *ICSBEP Handbook 2019*, Int. Crit. Saf. Benchmark Eval. Proj. Handb. Database (2019).
[31] R. J. McConn, C. J. Gesh, R. T. Pagh, R. A. Rucker, and I. I. I. Williams, Compendium of Material Composition Data for Radiation Transport Modeling, No. PNNL-15870 Rev. 1, Pacific Northwest National Lab. (PNNL), Richland, WA (United States), 2011.
[32] P. Helgesson, D. Rochman, H. Sjöstrand, E. Alhassan, and A. Koning, *UO2 versus MOX: Propagated Nuclear Data Uncertainty for Keff, with Burnup*, Nucl. Sci. Eng. **177**, 321 (2014).
[33] T. Yamamoto and Y. Kanayama, *Lattice Physics Analysis of Burnups and Isotope Inventories of U, Pu, and Nd of Irradiated BWR 9×9-9 UO2 Fuel Assemblies*, J. Nucl. Sci. Technol. **45**, 547 (2008).